

Supplementary Information

Efficient Encapsulation of CsPbBr₃ and Au nanocrystals in Mesoporous Metal–Organic Frameworks Towards Synergetic Photocatalytic CO₂ Reduction

Jia-Nan Huang, Yu-Jie Dong, Hai-Bing Zhao, Hong-Yan Chen, Dai-Bin Kuang and Cheng-Yong Su**

MOE Key Laboratory of Bioinorganic and Synthetic Chemistry, Lehn Institute of Functional Materials, School of Chemistry, Sun Yat-sen University, Guangzhou 510006, P. R. China.

E-mail: chenhy33@mail.sysu.edu.cn; cesscy@mail.sysu.edu.cn

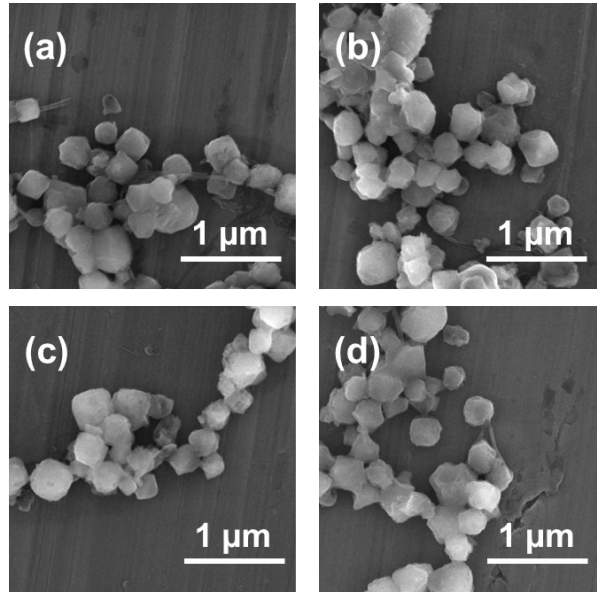


Figure S1. SEM image of (a) PCN-333(AI), (b) Au/PCN-333(AI), (c) CsPbBr₃/PCN-333(AI) and (d) CsPbBr₃/Au/PCN-333(AI).

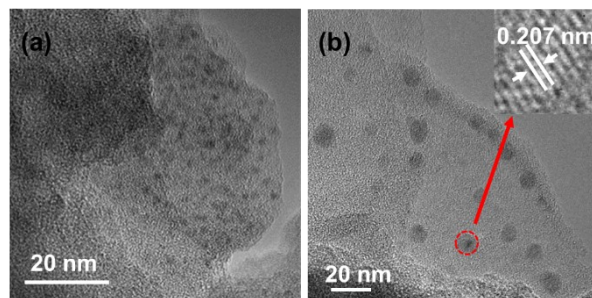


Figure S2. (a) TEM image of Au/PCN-333(AI). (b) TEM image of CsPbBr₃/PCN-333(AI).

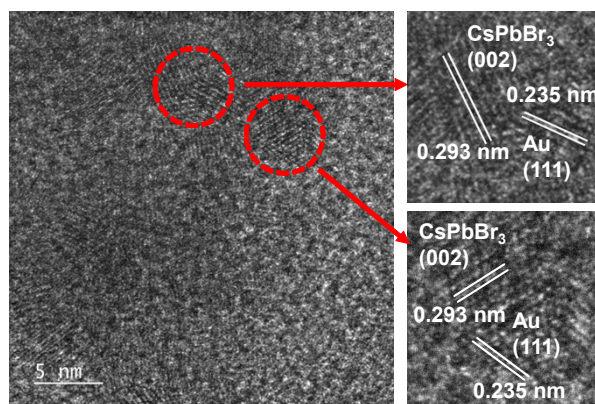


Figure S3. High resolution ultrathin section TEM image of CsPbBr₃/Au/PCN-333(AI).

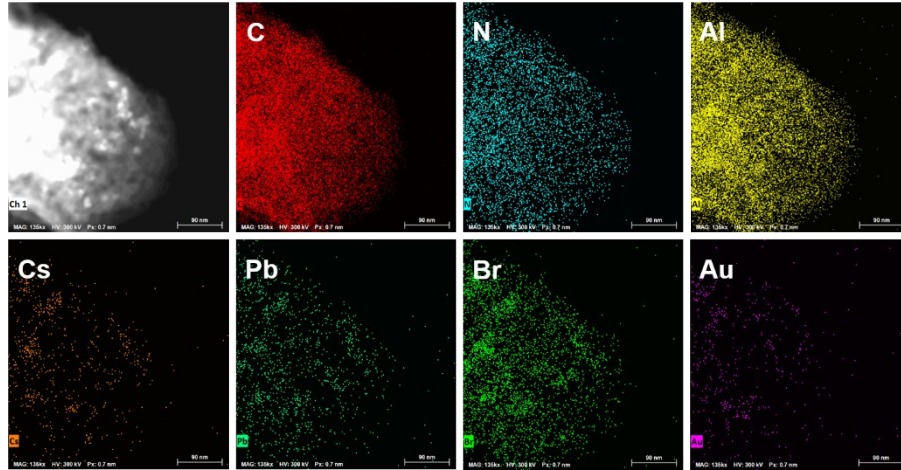


Figure S4. The elemental mapping images of CsPbBr₃/Au/PCN-333(Al).

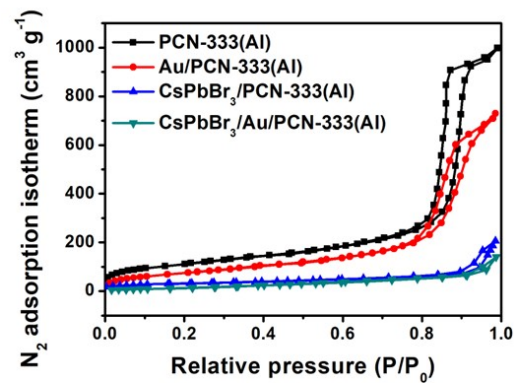


Figure S5. N₂ sorption isotherms of different samples at 77 K and 1 atm.

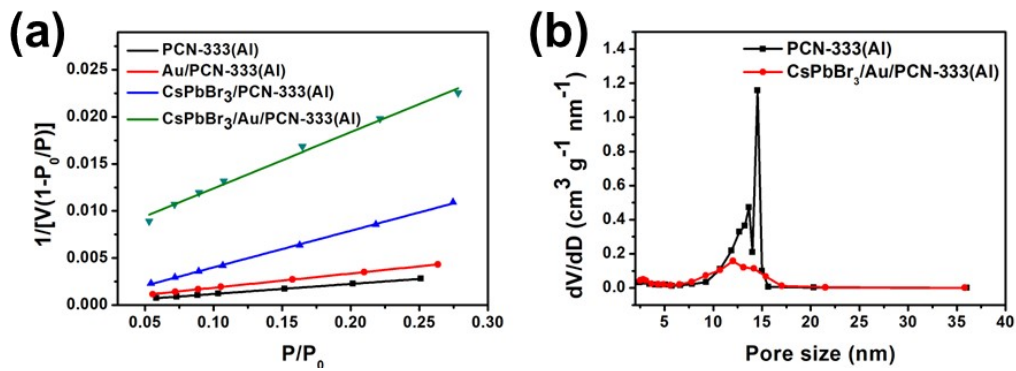


Figure S6. (a) The linear BET equation fitting results of different samples. (b) Comparison of DFT pore size distributions before and after encapsulating the Au and perovskite (obtained from N₂ sorption isotherm at 77 K and 1 atm).

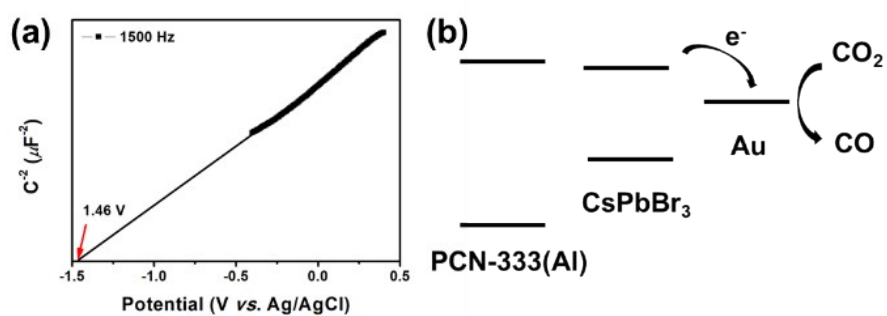


Figure S7. (a) Mott-Schottky plot of PCN-333(Al). (b) Schematic diagram of the relative energy band position of PCN-333(Al), CsPbBr₃ and Au.

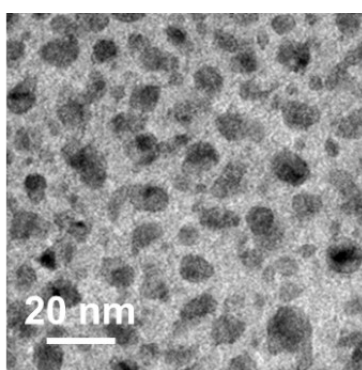


Figure S8. TEM image of CsPbBr₃ nanocrystals.

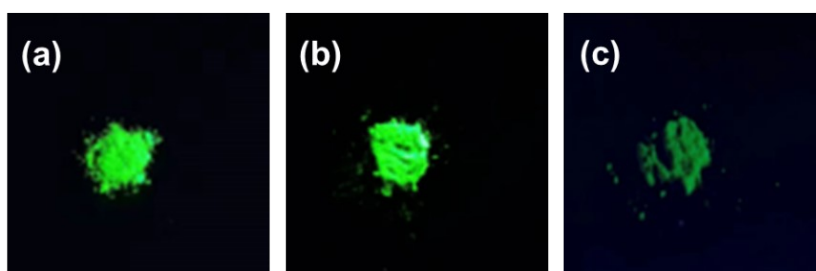


Figure S9. Photographs of samples excited at 365 nm: (a) CsPbBr₃ NCs, (b) CsPbBr₃/PCN-333(Al); (c) CsPbBr₃/Au/PCN-333(Al).

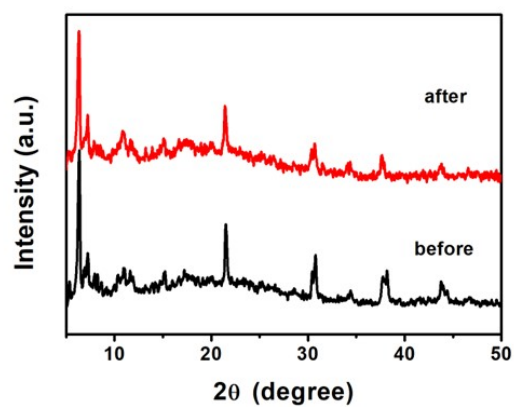


Figure S10. XRD pattern of CsPbBr₃/Au/PCN-333(Al) after 5 photocatalytic cycles.

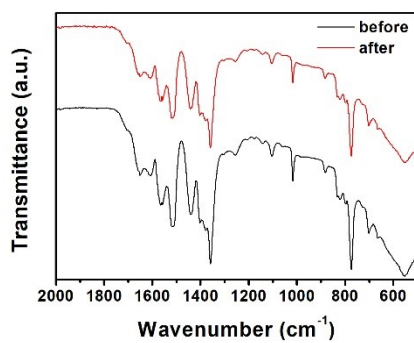


Figure S11. FTIR spectra of CsPbBr₃/Au/PCN-333(Al) before and after 5 photocatalytic cycles.

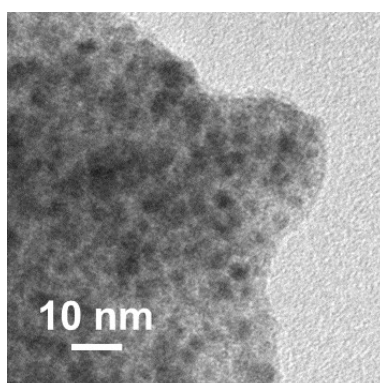


Figure S12. TEM image of CsPbBr₃/Au/PCN-333(Al) after 5 photocatalytic cycles.

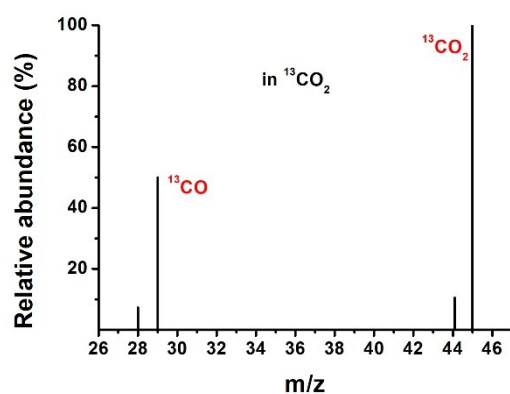


Figure S13. GC-MS spectra of isotope labeling catalytic products within $^{13}\text{CO}_2$ atmosphere.

Table S1. The content of each component in the composite sample ICP-MS

Sample	Au/wt%	CsPbBr ₃ /wt%
Au/PCN-333(Al)	5.8	-
CsPbBr ₃ /PCN-333(Al)	-	44.8
CsPbBr ₃ /Au/PCN-333(Al)	3.1	43.2

Table S2. Fitted PL decay parameters of CsPbBr₃, CsPbBr₃/PCN-333(Al) and CsPbBr₃/Au/PCN-333(Al).

Sample	τ_1/ns	$A_1/\%$	τ_2/ns	$A_2/\%$	$\tau_{\text{average}}/\text{ns}$
CsPbBr ₃ NCs	6.63	44.38	69.97	55.62	41.86
CsPbBr ₃ /PCN-333(Al)	6.15	44.48	52.61	55.52	31.94
CsPbBr ₃ /Au/PCN-333(Al)	0.44	65.74	16.06	34.26	5.79

Table S3. Summary of photocatalytic performances of different catalysts after 3 h of reaction.

	Condition	$Yield_{CO}$ / $\mu\text{mol g}^{-1}$	$Yield_{CH_4}$ / $\mu\text{mol g}^{-1}$	R_{electron}^a / $\mu\text{mol g}^{-1} \text{h}^{-1}$
No catalyst	CO ₂	-	-	-
No light	CO ₂	-	-	-
PCN-333(Al)	CO ₂	-	-	-
Au/PCN-333(Al)	CO ₂	-	-	-
CsPbBr ₃ NCs	CO ₂	7.41	2.22	10.83
CsPbBr ₃ /PCN-333(Al)	CO ₂	28.65	6.48	36.38
CsPbBr ₃ /Au/PCN-333(Al)- low CsPbBr ₃ loading	CO ₂	101.85	-	67.89
CsPbBr ₃ /Au/PCN-333(Al)	CO ₂	186.15	-	124.10
	N ₂	8.49	0.17	6.12

$$^a R_{\text{electron}} = [2Yield_{CO} + 8Yield_{CH_4}] / \text{Time}$$